Modeling of Thermodynamic Properties for Bcc, Fcc, Liquid, and Amorphous Iron

Qing Chen and Bo Sundman

The thermodynamic properties of pure iron have been analyzed by using models that contain some parameters of physical significance. In addition to the lattice, electronic, and magnetic components, a contribution to the heat capacity due to the excitation between two magnetic states has been considered for the fcc phase. The liquid and amorphous phases have been treated as one phase with the generalized two-state model. The magnetic properties of amorphous iron have been reviewed and taken into account in the modeling. A relatively more accurate description of the magnetic effect in the bcc phase has been obtained; this is found to be essential for the accommodation of various experimental measurements on the enthalpy and Gibbs energy differences between bcc and fcc iron.

Introduction

The present investigation of the thermodynamic data of iron is motivated by the recommendations put forward at the Ringberg 95' workshop [1995Sun, 1995Cha, 1995Ågr, 1995Fon], where it was suggested that the thermodynamic functions for elements and other end members of solutions should be described by models accounting for different physical effects rather than by simple mathematical polynomials. With such models, some of the model parameters will have clear physical meaning, and the derived values can be checked against known experimental or theoretical information. Another reason for adopting such models in the CALculation of PHAse Diagrams (CALPHAD) field [1970Kau, 1998Hil, 1998Sau] is that the extrapolation of thermodynamic properties from the stable to metastable region can be carried out with more confidence, and parameters for metastable phases can be estimated with better chance of success. The use of such models is not new. As a matter of fact, it has been tried on different substances long before the name CALPHAD was coined. This is especially true for iron, an element of tremendous interest for industrial application and theoretical study.

[1955Zen] was the first who tried to divide the lattice stability into a magnetic and a nonmagnetic contribution. Shortly after this attempt, [1956Wei] resolved the thermodynamic functions further into their magnetic, lattice, and electronic components on the basis of additivity of the respective heat-capacity components. Following the latter approach, [1963Kau] and [1982Ben] have considered the contribution resulting from the excitation between two magnetic states for fcc iron and reanalyzed the lattice stability data.

In spite of the attractiveness of physical approaches, empirical methods have gained wide use [1991Din] due to their simplicity. To represent the nonmagnetic contribution

to the Gibbs energy of various phases of iron, [1979Ågr] and [1985Gui] have employed the well-known Meyer-Kelley polynomial form. The resultant mathematical descriptions can satisfactorily reproduce most of the experimental data in the unary Fe and binary Fe-C and Fe-N systems. In their investigations, both [1979Ågr] and [1985Gui] noticed that, after they accepted [1967Orr]'s value on the Gibbs energy difference between bcc and fcc iron at 1000 K, the optimized transformation enthalpy at 1185 K was outside the experimental error limits. [1985Gui] speculated that an even more ambitious treatment of the magnetic contribution in bcc iron might be needed. Another concern [1994Gho] about the empirical approach is that the extrapolated low-temperature stability data for bcc and fcc iron may involve large uncertainties.

In addition to the previously mentioned efforts, there exist a large number of reviews and tabulations of the thermodynamic data for iron [1932Aus, 1937Joh, 1946Zen, 1949Fis, 1951Dar, 1962And, 1963Koh, 1963Hul, 1967Orr, 1973Hul, 1979Sch, 1986Des]. Among these, [1967Orr] appears to have the highest quality of precision, consistency, and reliability of its tabulations; this was demonstrated in a subsequent thermodynamic evaluation of the Fe-C phase diagrams [1972Chi]. [1967Orr]'s work was later accepted totally in [1973Hul]'s compilation. The most recent review by [1986Des] presents similar results on the thermodynamic functions for the stable iron phases, but it makes no efforts to estimate metastable properties.

In this work, we will use models in line with the recommendations from [1995Sun, 1995Cha, 1995Ågr, 1995Fon] and analyze the thermodynamic properties for bcc, fcc, liquid, and amorphous iron on the basis of available critical assessments from [1985Gui] and [1967Orr]. We will demonstrate that with a relatively more accurate description of the magnetic heat capacity of bcc iron, one cannot only adopt the well-assessed value of the 1000 K Gibbs energy difference but also accept the preferred values on the 1185 K transformation enthalpy. Furthermore, the agreement between calculated and experimental thermodynamic information will be improved over an extended temperature range. It should be

Qing Chen and **Bo Sundman,** Department of Materials Science and Engineering, Royal Institute of Technology, SE-100 44, Stockholm, Sweden. Contact e-mail: qing@met.kth.se.

mentioned that the lattice stability of the high pressure form of iron, *i.e.*, the hcp phase is also very important, but this will be covered in another paper on a reassessment of the T-P diagram of iron using the models presented in this work.

Thermodynamic Models

Bcc Phase

According to [1995Cha, 1995Fon, 2000Che], the heat capacity of the bcc phase can be represented by

$$C_P = 3R\left(\frac{\Theta_E}{T}\right)^2 \frac{e^{\Theta_E/T}}{(e^{\Theta_E/T} - 1)^2} + aT + bT^4 + C_P^{\text{mag}} \quad \text{(Eq 1)}$$

where the first term is the contribution from the harmonic lattice vibration, and θ_E is the Einstein temperature. The second term consists of contributions from the electronic excitations and low-order anharmonic corrections (dilatational and explicitly anharmonic), and the parameter, a, can be related to nonthermodynamic information, *e.g.*, the electron density of states at the Fermi level. The third term is from the high-order anharmonic lattice vibrations, and it is seldom that one can find experimental information to validate the parameter, b. The reason for the choice of T^4 [2000Che], rather than T^2 [1995Cha] in the third term, is that the former one gives better fit to the high-temperature heat-capacity data for a wide spectrum of pure elements, and, most importantly, it results in reasonable values for the parameter, a, while the latter one does not [2000Che]. The last term in Eq 1 denotes the contribution from the magnetic transformation and is described by using the model from [1976Ind] in the form of [1978Hil]'s approximation with a slight change of the parameters involved and the number of terms retained in the truncation (Appendix). As we shall see later, this adjustment, which leads to a better reproduction of the magnetic heat-capacity data for the bcc phase, makes it possible for us to accept the preferred values of both the 1185 K transformation enthalpy and the 1000 K Gibbs energy difference between bcc and fcc iron.

From the expression for C_P, the Gibbs energy at 101,325 Pa can be evaluated:

$$G = E_0 + \frac{3}{2}R\theta_E + 3RT \ln\left[1 - \exp\left(-\frac{\theta_E}{T}\right)\right] - \frac{a}{2}T^2$$

$$- \frac{b}{20}T^5 - \int_0^T\left[\int_0^T \frac{C_P^{\text{mag}}}{T}dT\right]dT \quad \text{(Eq 2)}$$

where E_0 is the total energy of the ferromagnetic bcc structure at 0 K, and the second term is the energy of zero-point lattice vibration [1954Bor, 1986Gri]. The preceding equation uses the ferromagnetic ground state as the reference state and treats the magnetic contribution as a magnetic disordering effect. While this choice is natural, it can lead to unrealistic miscibility gaps in alloy systems where the other components

have paramagnetic ground states [1991Ind]. As a result, in practice one always uses the (hypothetical) paramagnetic ground state as the reference state and treats the magnetic contribution as a magnetic ordering effect. This is easily done by rewriting Eq 2 as

$$G = G^{fm} - \int_0^\infty\left[\int_0^\infty \frac{C_P^{\text{mag}}}{T}dT\right]dT - \int_0^T\left[\int_0^T \frac{C_P^{\text{mag}}}{T}dT\right]dT$$

$$+ \int_0^\infty\left[\int_0^\infty \frac{C_P^{\text{mag}}}{T}dT\right]dT$$

$$= (G^{fm} + G^{\text{mdo}}(\infty)) + (G^{\text{mdo}} - G^{\text{mdo}}(\infty))$$

$$= G^{pm} + G^{mo} \quad \text{(Eq 3)}$$

where G^{fm} and G^{pm} are the Gibbs energy of ferromagnetic and paramagnetic states, respectively, $G^{\text{mdo}}(\infty)$ is the total Gibbs energy for magnetic disordering, and G^{mo} is the Gibbs energy for magnetic ordering. The expressions of $G^{\text{mdo}}(\infty)$ and G^{mo} are given in the Appendix.

It is well known [1987And] that a direct extrapolation of the Gibbs energy for a solid phase beyond its melting point may lead to absurd results. For example, the solid phase may be predicted to be stable again at temperatures far above the melting point. To avoid this problem, the following empirical expression [2000Che] is adopted for the bcc phase above its melting temperature:

$$C_P = 3R\left(\frac{\Theta_E}{T}\right)^2 \frac{e^{\Theta_E/T}}{(e^{\Theta_E/T} - 1)^2} + a' + b'T^{-6} + c'T^{-12}$$

$$+ C_P^{\text{mag}} \quad \text{(Eq 4)}$$

$$G = \frac{3}{2}R\theta_E + 3RT \ln\left[1 - \exp\left(-\frac{\theta_E}{T}\right)\right] + H' - S'T$$

$$+ a'T(1 - \ln T) - \frac{b'}{30}T^{-5} - \frac{c'}{132}T^{-11}$$

$$+ G^{\text{mdo}}(\infty) + G^{mo} \quad \text{(Eq 5)}$$

where a', b', and c' are determined by the heat capacity and its derivative of the bcc phase at the melting temperature and by requiring that C_P should equal the value of the liquid phase at an arbitrarily chosen high temperature, T_h. The parameters H' and S' are then calculated from the values on the enthalpy and entropy of the bcc phase at the melting point. Comparing Eq 4 and 5 with Eq 1 through 3, we know that those parameters can be calculated analytically from optimized E_0, θ_E, a, b, and $C_P^{\text{mag}}(T_h)$ in Eq 1 and 2. The exact mathematical expressions were given in [2000Che]. The proposed Eq 4 and 5 ensure that the heat capacity of the bcc phase nearly coincides with the value chosen for the liquid phase at high temperatures while maintaining continuity in both the solid heat capacity itself and its first derivative at the melting point. This new method is simple and easy to apply and avoids the kink in the C_P curve inherent in the previous extrapolation method [1987And].

Fcc Phase

Both Mössbauer experiments [1988Car, 1989Ken] and total energy calculations [1993Asa, 1999Her] have confirmed [1963Wei] and [1963Kau]'s postulation that fcc iron exists in a low moment-low volume antiferromagnetic ground state and a high moment-high volume ferromagnetic state. The excitation between these two states yields an additional contribution to the Gibbs energy, and it is this contribution that makes it possible for fcc iron to turn stable at 1185 K [1963Kau, 1982Ben, 1991Kau]. The two-magnetic states effect can be described using the Schottky model [1963Wei, 1963Kau, 1970Mio, 1977Mio]:

$$G^{2st} = -RT \ln \left[1 + \frac{g_2}{g_1} \exp \left(-\frac{\Delta E^{2st}}{RT} \right) \right] \qquad \text{(Eq 6)}$$

where ΔE^{2st} is the energy gap between the two states; the term g_2/g_1 denotes the degeneracy ratio of the two states.

The other contributions to the Gibbs energy are expressed in the same way as that for the bcc phase, Eq 1 through 5. In this case, for the magnetic contribution, the Néel temperature, T_N, is used instead of the Curie temperature, T_C (Appendix). The values for the Néel temperature, T_N, and average magnetic moment per atom, β, are taken to be 67 K and 0.7 μ_B [1991Din].

The extrapolation of the Gibbs energy of fcc iron above the melting point is similar to that of bcc iron except that the two-magnetic states contribution is added in Eq 5.

Liquid and Amorphous Phases

The liquid and amorphous phases have been described using the so-called generalized two-state model [1995Ågr, 1988Ågr], where they are treated as one phase in which the atoms can be in either the amorphous-like state or liquidlike state. With this model, it is possible to represent the continuous change of properties from the amorphous phase at low temperatures to the liquid phase at high temperatures. As a result, the liquid and amorphous phases will simply be called the liquid-amorphous phase in this study, and their Gibbs energy shall be denoted G^{liq-am}. According to [1988Ågr], the Gibbs energy of the liquid-amorphous phase can be written as

$$G^{liq-am} = {}^\circ G^{am} - RT \ln[1 + \exp(-\Delta G_d/RT)] \qquad \text{(Eq 7)}$$

where $\Delta G_d = {}^\circ G^{liq} - {}^\circ G^{am}$ and the quantities ${}^\circ G^{am}$ and ${}^\circ G^{liq}$ can be thought of as the Gibbs energy of the system where all the atoms are in the amorphous-like state and liquidlike state, respectively. The representation of ${}^\circ G^{am}$ is the same as that of the bcc phase except that the high-order anharmonic vibrational contribution is excluded [2000Che]. This may be justified by the fact that only very weak long-range interatomic interactions exist in the ideal amorphous state. The Gibbs energy difference between the liquidlike state and the amorphous-like state is expressed by

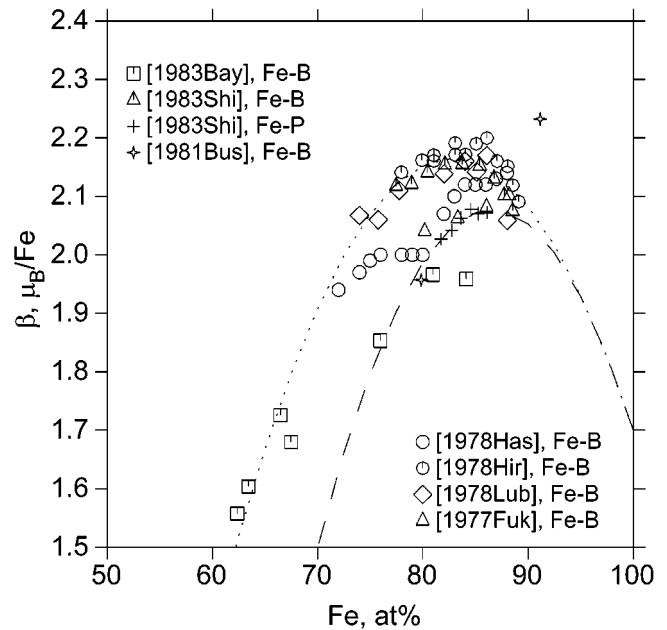$$\Delta G_d = A + BT + CT \ln T \qquad \text{(Eq 8)}$$

Fig. 1 Composition dependence of the experimental magnetic moment in binary Fe-B and Fe-P amorphous alloys

The absolute value of B in the preceding equation should not be too much different from that of the communal entropy, R, the gas constant [1995Ågr, 1988Ågr]. In practice, we found that it is better to simply assume that the absolute value of B equals the entropy of melting because of its extreme sensitivity to the experimental heat-capacity data chosen for the parameter optimization [2000Che].

Amorphous iron is ferromagnetic at low temperatures [1993Gri, 1996Lie]. In order to describe the magnetic contribution to its Gibbs energy, we have to know its Curie temperature and magnetic moments. In the next section, a brief review of the experimental results on the magnetic properties of amorphous iron is presented.

Magnetic Properties of Amorphous Iron

Essentially pure amorphous iron has recently been prepared by [1991Sus, 1995Bel, 1993Gri, 1993Bel, 1998Lon] using sonochemical methods. A Mössbauer effect study [1998Lon] suggests that amorphous iron has a magnetic moment of $1.7\mu_B$ at 295 K. This value agrees well with those, $1.4\mu_B$ and $1.7\mu_B$, derived earlier from neutron diffraction measurements [1993Bel] and magnetization measurements [1993Gri], respectively. Moreover, recent *ab initio* linear muffin-tin atomic-sphere approximation calculations [1996Lie] yielded a 295 K moment of $1.8 \pm 0.4\mu_B$ for amorphous iron. Another support for the acceptance of $1.7\mu_B$ is shown in Fig. 1 and 2, where the extrapolation of amorphous alloy data to pure amorphous iron can be rationalized using this value. As can be easily seen, the experimental data are widely scattered and sometimes the variation trend is completely opposite, for example, the measurements of [1980Mas] and [1985Lio] for the Fe-Hf alloys in Fig. 2. In this situation, different extrapolation
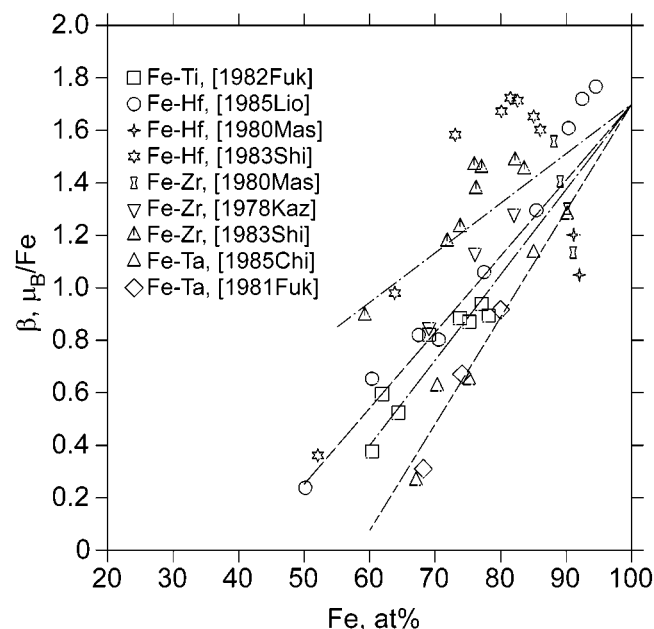
Fig. 2 Composition dependence of the experimental magnetic moment in binary Fe-TM amorphous alloys

Fig. 3 Composition dependence of the experimental Curie temperature in binary Fe-based amorphous alloys

methods can be used for different sets of data. This is why there are so many conflicting estimates [1985Cow] about the magnetic moment of pure amorphous iron.

Amorphous iron is ferromagnetic, according to the magnetization measurements of [1993Gri]. Applying the mean-field theory [1996Kit], [1993Gri] calculated the Curie temperature with use of the effective exchange constant, determined by analyzing the magnetization results according to Block's law [1996Kit]. They predicted that the Curie temperature is about 480 K. However, a careful examination of the equation they used for their calculation reveals that a term, $(Q_c/Q_a)^{2/3}$, was missing. Here, Q_c and Q_a are the numbers of atoms in conventional bcc and amorphous unit cells, respectively. Following [1993Gri]'s assumption that the amorphous phase is locally close packed and has a coordination number of 12, one has $Q_a \approx 4$. Since $Q_c = 2$, their predicted Curie temperature (480 K) should be lowered by multiplying by $(1/2)^{2/3}$, *i.e.*, $T_C = 302$ K. On the other hand, [1993Gri] has also placed 580 K as a lower limit on T_C because their measured TGA curve exhibited no features until 585 K, where the crystallization of amorphous iron occurred. However, as [1993Gri]'s TGA measurements were only shown above 373 K, it is not clear whether the TGA experiment was also carried out below 373 K, where the magnetic transformation probably takes place according to our recalculation. As a matter of fact, extrapolations of Fe-based amorphous alloy data to pure iron all suggest that the Curie temperature, T_C, of amorphous iron should be below 373 K. For instance, [1976Hei] claimed that $T_C = 270$ K from experimental information on the Fe-rare-earth systems; [1981Chi] suggested that $T_C = 298$ K from the measurements on the Fe-B system; [1984Ega] obtained $T_C = 320$ K from the data on amorphous Fe-metalloid; and [1985Lio, 1985Chi] reported $T_C = 200$ K from the data on amorphous Fe-Hf and Fe-Ta alloys. The disagreements among these estimations are due to experimental errors and
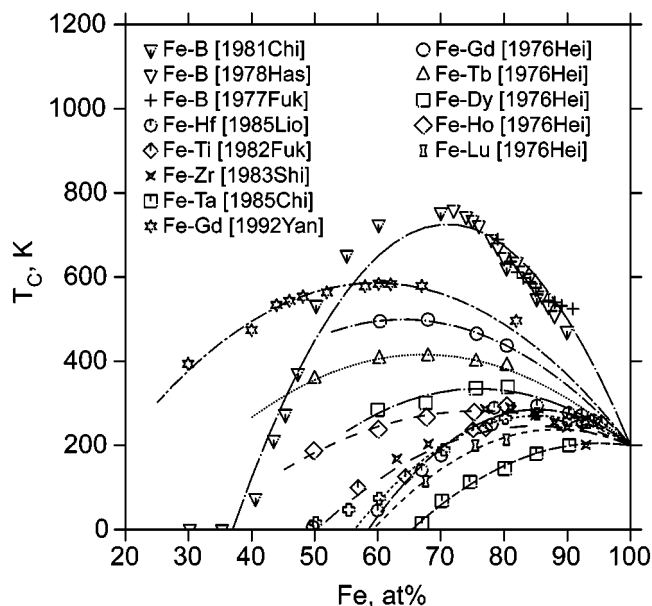
the differences in data extrapolation methods. In Fig. 3, the measured Curie temperatures of different amorphous alloys have been plotted together against the atomic concentration of Fe. It is shown that nearly all the information, except that of [1983Shi], can be accounted for by choosing $T_C = 200$ K for pure amorphous iron and applying parabolic fit.

From the preceding discussion of the experimental information, we may conclude that it is reasonable for us to adopt $T_C = 200$ K and $\beta = 1.7 \mu_B$ for the description of the magnetic contribution to $^\circ G^{am}$, the Gibbs energy of iron in the ideal amorphous state. As amorphous iron is assumed to be locally close packed, the short-range order fraction of enthalpy, p, has been taken to be 0.25, the same as that for fcc phases (Appendix).

Parameter Determination

Since its thermodynamic functions are well defined, the bcc phase was examined first. Then, we used the selected data on the enthalpies of phase transformations and some other nonthermodynamic information to fix parameters for the fcc phases. Finally, the liquid and amorphous phase was treated. The PARROT module [1984Jan] in the Thermo-Calc software package [1985Sun] has been used for parameter optimization.

Bcc Phase

The assessed entropy data [1985Gui] for the bcc phase from room temperature to its melting point were used as the "experimental" input to fix the parameters θ_E, a, and b in Eq 1 and 2. The value of E_0 in Eq 2 was evaluated by taking the room-temperature enthalpy as reference, *i.e.*, setting $H^{bcc}_{298.15}$ to 0.

The parameters for the empirical description of the bcc

phase above the melting temperature were calculated using the newly assessed data on C_P, dC_P/dT, H, and S at 1811 K and one C_P value, the same as that of the liquid phase [1985Gui] at an arbitrarily chosen high temperature, 4000 K.

Fcc Phase

The enthalpies of phase transformation at 1185 and 1667 K are well determined by [1960Wal, 1963Den, 1965Bra, 1980Rog] using adiabatic calorimetry and are accepted in [1967Orr] and [1973Hul]'s work. However, since the information on the enthalpy and entropy data at these two temperatures is not sufficient to fix six parameters (E_0, θ_E, a, b, ΔE^{2st}, and g_2/g_1) for the fcc phase, we first have to determine two parameters from other nonthermodynamic experiments or considerations.

Using the Lindemann's rule and taking the melting temperature of the fcc Fe to be about 1800 K, [1963Kau] found that the fcc phase has about the same high-temperature entropy-Debye temperature θ_D (0) as the bcc phase does. The notation θ_D (0) is a special case of the Debye temperatures θ_D (n), which are derived from the nth moment of the phonon frequencies [1986Gri]. In an ideal Debye solid, all θ_D (n) are equal to the ordinary Debye temperature, θ_D (−3), obtained from low-temperature heat capacity or elastic constant data. In a real solid, θ_D (0) is different from θ_D (−3), and the ratio between them appears to be constant but different for different groups of elements [2001Che]. In an attempt to analyze the Gibbs energy of iron, [1974Gri] reported that the difference of θ_D (0) between the fcc and bcc phases is about 1%. Extrapolation of the experimental elastic constant data of fcc Fe-Ni alloys to pure iron also suggested that the low-temperature limit of the Debye temperature θ_D (−3) is about the same for fcc and bcc iron [1971Tan, 1975Hau]. Assuming they have the same θ_D (0)/θ_D (−3) ratio [2001Che], fcc and bcc iron, thus, have about the same θ_D (0). Therefore, it is reasonable to choose the same value of θ_E, which is proportional to θ_D (0) [1954Bor, 1997Cac], for fcc iron as that for bcc iron.

The degeneracy ratio of the two magnetic states, g_2/g_1, determined from experimental heat-capacity data [1978Ben] for various $Fe_{50}Ni_xMn_{50-x}$ alloys, has recently been plotted against electron concentrations and extrapolated to pure iron by [1994Ace]. The obtained value, 1.35, was then used successfully to account for the thermal expansion of the fcc Fe. Before we accepted this value, we actually tried to optimize the parameters E_0, a, b, ΔE^{2st}, and g_2/g_1 simultaneously by using the transformation enthalpy and entropy data and the extrapolated values on the enthalpy difference between the fcc and bcc phases at 673 and 773 K from [1960Sch]. The value of g_2/g_1 obtained in this way is too large (3.37) compared with the maximum value (1.9) suggested by [1963Wei] from theoretical considerations, and the resultant a is too small (2.3 × 10⁻³ J/mol/K⁻²) compared with the value (5.02 × 10⁻³ J/mol/K⁻²) suggested for the electronic contribution by [1964Gup]. In a similar assessment, where the heat capacity data for the fcc phase by [1960Wal] and [1962And] were also used for parameter optimization, [1963Kau] obtained the reasonable values of 5.02 × 10⁻³ J/mol/K⁻² for

a and 1.79 for g_2/g_1. However, they did not consider the low-temperature antiferromagnetic contribution for the fcc phase. If it had been considered, the resultant parameters would have also been unacceptable. As a result, we finally accepted 1.35 for g_2/g_1 from [1994Ace] and found that the optimized a was then in good agreement with the experimental data [1964Gup].

The description of the fcc phase above the melting point was obtained in a similar way as that for the bcc phase.

Liquid-Amorphous Phase

The effective Mössbauer temperature, θ^M, a quantity that is about the same as the low-temperature limit of the Debye temperature θ_D (−3) [1986Gri], has been determined for amorphous iron by [1998Lon]. The observed value is 377 K, in fair agreement with the value of 350 K predicted from molecular dynamics [1992Gup] and the value of 345 K reported for nanostructured iron [1987Her]. Assuming that the ratio between θ_D (−3) and the high-temperature entropy-Debye temperature θ_D (0) is the same for fcc and amorphous structures, we have $\theta(0)$ = 343 K, and the corresponding Einstein temperature θ_E (≈0.714 θ_D (0) [1997Cac]) is, thus, about 245 K. This value was used in this study for describing the harmonic vibration of the ideal amorphous state.

The remaining parameters, a and E_0 for representing °G^{am} in Eq 1 and 2 and A and C in Eq 8, are optimized using the assessed data [1985Gui] on the enthalpy and entropy of melting and the heat capacities at and above the melting point.

Results and Discussion

All the parameters obtained in this work are listed in Table 1. The obtained θ_E and a are compared with other nonthermodynamic information in Table 2. The agreement is good.

Figure 4 shows the calculated heat capacity of bcc, fcc, and liquid-amorphous iron in their stable and metastable temperature ranges. Comparisons with experimental data are given in Fig. 5 and 6. For the bcc phase, the agreement is very good over the entire temperature range except in the region of very low temperatures, where the Einstein model is known to be inadequate [1986Gri, 1996Kit]. For the fcc phase, the calculated values coincide almost exactly with those determined by [1960Wal, 1972Sal, 1974Cez], although they were not used in the parameter optimization.

Above the melting point of bcc iron, the heat capacities of the solid phases can be seen in Fig. 4 to approach smoothly to a constant value for the liquid phase from [1985Gui]. This constant value can be viewed as an average one for the liquid phase over the temperature range not far from its point of solidification. It is interesting to note that the calculated liquid heat capacity is predicted first to drop slightly above the melting point and then to increase gradually at higher temperatures. For the undercooled iron liquid, its heat capacity increases for a short while and then drops until the magnetic ordering effect takes control. So far, the large uncertainties of the available experimental measurements preclude a determination of such kind of behavior for liquid iron, although the
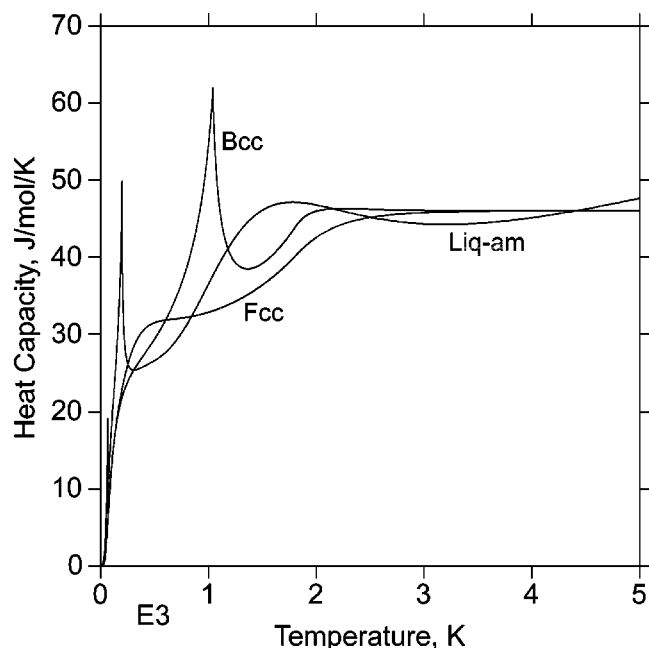
Fig. 4 The calculated heat capacity of iron

Fig. 5 Comparison between the calculated and experimental heat capacity of iron above room temperature

Table 1   Summary of the Gibbs energy expressions for iron at $P = 101{,}325$ Pa

Bcc

$T_C = 1043$, $\beta = 2.22$, $p = 0.37$
$-8.41026596E{+}03 - 3.2390815E{-}03*T^{**}2 - 3.3191338E{-}14*T^{**}5$
$+ \text{GEIN}(3.09E{+}02) + \text{GMDO}(\infty) + \text{GMO}$ $0.0 < T < 1811.00$

$-3.32084173E{+}04 + 1.6540504E{+}02*T - 2.10474823E{+}01*T^*\ln(T)$
$-2.7818280E{+}18*T^{**}({-}5) + 4.2811788E{+}37*T^{**}({-}11)$
$+ \text{GEIN}(3.09E{+}02) + \text{GMDO}(\infty) + \text{GMO}$ $1811.00 < T < 6000.00$

Fcc

$T_N = 67$, $\beta = 0.70$, $p = 0.25$
$-2.61500904E{+}03 - 2.7933375E{-}03*T^{**}2 - 2.1239087E{-}14*T^{**}5$
$+ \text{GEIN}(3.09E{+}02) + \text{G2ST}(9.02352375E{+}03 - 2.49522260E$
$+ 00*T) + \text{GMDO}(\infty) + \text{GMO}$ $0.0 < T < 1811.00$

$-3.23895438E{+}04 + 1.6831394E{+}02*T - 2.09834791E{+}01*T^*\ln(T)$
$+9.2444598E{+}18*T^{**}({-}5) - 1.4750509E{+}37*T^{**}({-}11)$
$+ \text{GEIN}(3.09E{+}02) + \text{G2ST}(9.02352375E{+}03 - 2.49522260E{+}00*T)$
$+ \text{GMDO}(\infty) + \text{GMO}$ $1811.00 < T < 6000.00$

Liquid-amorphous

$T_C = 200$, $\beta = 1.70$, $p = 0.25$
$+7.10320801E{+}03 - 1.9730116E{-}03*T^{**}2 + \text{GEIN}(2.45E{+}02)$
$+ \text{G2ST}(4.27549478E{+}04 - 7.62400000E{+}00*T$
$- 1.08230446E{+}00*T^*\ln(T))$
$+ \text{GMDO}(\infty) + \text{GMO}$ $0.0 < T < 6000.00$

Auxiliary functions

$\text{GEIN}(\theta) = 1.5*R*\theta + 3*R*T^*\ln(1 - \exp(-\theta/T))$
$\text{G2ST}(\Delta G) = -RT^*\ln(1 + \exp(-\Delta G/RT))$

Note: All values are in SI units. The Gibbs energy data are given relative to the enthalpy of bcc phase at 298.15 K and 101,325 Pa. The expressions for GMDO(∞) and GMO are given in Eq A9 and A10

Table 2   Comparison between optimized and experimental data on the Einstein temperature and electronic heat-capacity coefficient for bcc and fcc iron

	Bcc		Fcc	
Source	θ_E, K	γ, mJ/mol/K^2	θ_E, K	γ, mJ/mol/K^2
[1996Kit]	...	4.98	...	...
[1981Sch1]	298(a)	...	...	...
[1971Mar]	...	4.72	...	...
[1966Shi]	...	4.81	...	...
[1964Gup]	...	...	...	5.02
[1960Che]	...	4.979	...	...
[1959Arp]	...	4.90	...	...
[1956Hof]	309(a)	...	...	...
[1939Kee]	...	5.02	...	...
This work	309	6.48(b)	309	5.59(b)

(a) Converted from the reported $\theta_D(0)$
(b) The optimized value for a in Eq1, which consists of electronic contribution and low-order anharmonic vibrational contributions (dilatational and explicitly anharmonic)

same trend is well known for many low-melting substances [1991Din, 1984Per, 1967Che]. Taking a simple approach, previous assessments [1967Orr, 1985Gui, 1986Des] have all considered the heat capacity of liquid iron as a constant. In the present study, the liquid and amorphous phases have been
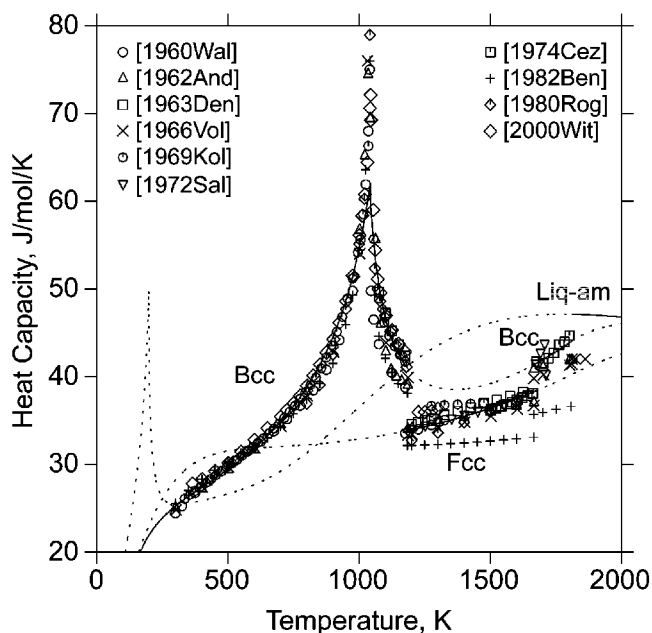
treated as one phase using a phenomenological generalized two-state model, which is ideal for the description of the temperature dependence of heat capacity experimentally found for substances with a strong tendency to form amorphous structure [1988Ågr, 1984Per, 1967Che]. If one allows the parameter, B, in Eq 8, corresponding to the entropy difference between the atoms in the liquidlike and amorphous-like states, to vary during the parameter optimization, a nearly constant value for the heat capacity above the melting point can be obtained, but then, the optimized value for B will be very different from that of the communal entropy, R [1995Ågr, 1988Ågr]. The calculated variation of the liquid
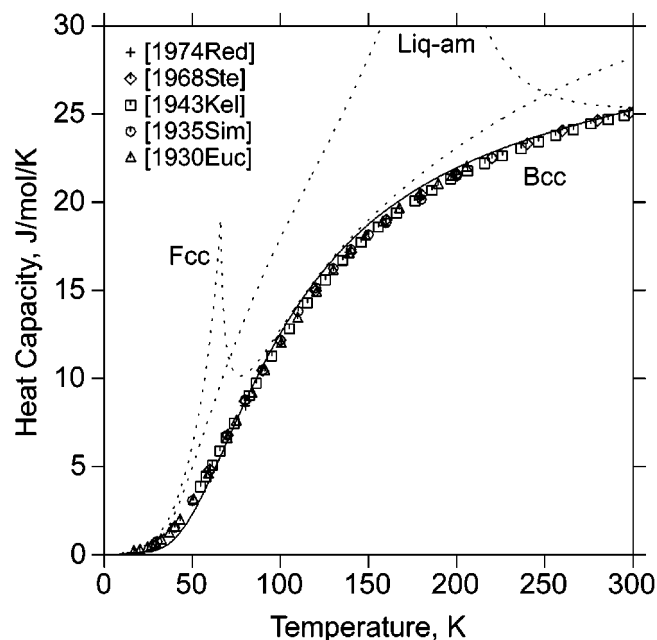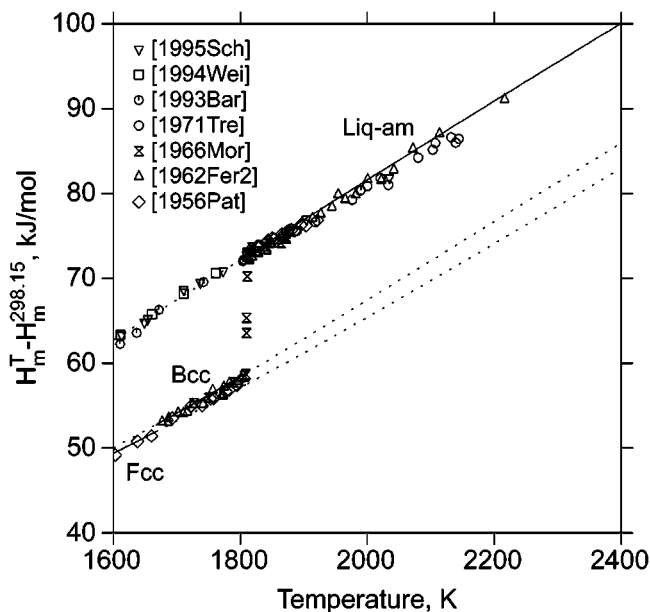
Fig. 6 Comparison between the calculated and experimental heat capacity of iron below room temperature

heat capacity with temperature shown in Fig. 4 is a consequence of fixing B to the melting entropy of bcc iron, and we believe that, in this way, not only the optimized parameters become more reasonable, but also the calculated results are probably closer to reality. As a matter of fact, the present prediction for the heat capacity of liquid iron is well within the large experimental uncertainties (46.632 ± 3.0 [1986Des]). Furthermore, [1994Wei] has reported that the heat capacity of liquid iron undercooled within 200 K is 5% larger than that of the liquid at the melting point. The agreement between the calculated and experimental heat contents of the liquid phase is shown in Fig. 7(a) and for the solid phases in Fig. 7(b).

The calculated transformation enthalpies of iron are compared with both experimental and assessment values in Table 3. It is easily seen that the preferred values [1963Den, 1965Bra, 1962Fer1, 1980Rog, 1967Orr, 1973Hul] are exactly reproduced in this study. In Fig. 8, we show an improved agreement between the calculations and measurements on $\Delta H^{\text{bcc/fcc}}$ over an extended temperature range. The comparison for $\Delta G^{\text{bcc/fcc}}$ is given in Fig. 9, and the agreement is excellent. From these pictures, we see clearly the consistency among adiabatic calorimetry measurements on the phase transformation enthalpy [1963Den, 1965Bra, 1980Rog], enthalpy differences derived from the Fe-C phase diagram [1946Smi], and the Gibbs energy difference derived from Fe-(Mo, Sb, Sn, W, Mn, and Ni) phase diagrams [1967Hil]. The high quality of [1967Orr]'s tabulation in the relevant temperature range is also evident in Fig. 8 and 9.

The success of the above reconciliation is due to the use of the modified treatment of the magnetic contribution (Appendix). A preliminary assessment using the original description [1976Ind, 1978Hil, 1985Gui] yielded the dashed line in Fig. 8 and 9, if the preferred value for phase transformation enthalpy at 1184 K was accepted. As can be easily

(a)
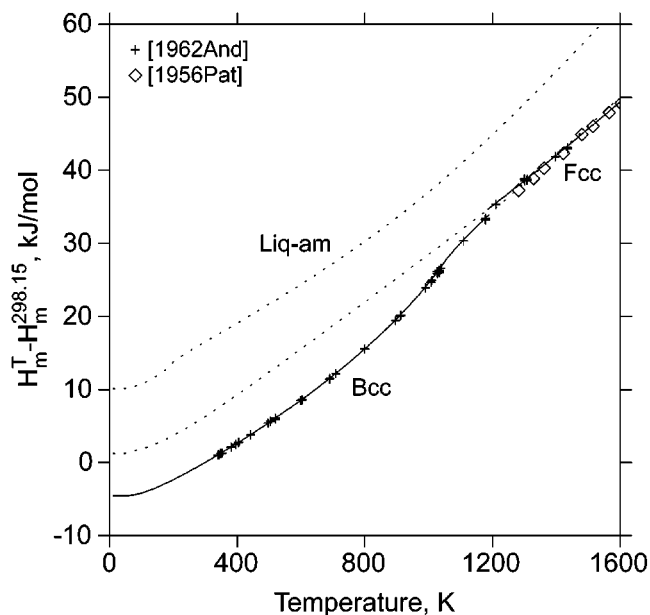
(b)

Fig. 7 Comparison between the calculated and experimental heat content of iron (**a**) above 1600 K and (**b**) below 1600 K

seen, those results are unacceptable because of the large discrepancies between the calculations and measurements at low temperatures. [1979Ågr] and [1985Gui] encountered this problem and placed more weight on [1967Orr]'s value for the Gibbs energy difference at 1000 K, which means that a larger phase-transformation entropy and, thereby, a large enthalpy at 1185 K must be used (the dotted line in Fig. 8 to 10). Apparently, in order to accommodate both the adiabatic calorimetry data on the enthalpy of phase transformation [1963Den, 1965Bra, 1980Rog] and the lower temperature enthalpy and Gibbs energy differences derived from the Fe-based phase-diagram information [1946Smi, 1967Hil], the

Table 3   Comparison between assessed and experimental enthalpies of phase transformation for iron

Source	$\Delta H^{bcc \rightarrow fcc}$ (1185 K), J/mol	$\Delta H^{fcc \rightarrow bcc}$ (1667 K), J/mol	$\Delta H^{bcc \rightarrow liq}$ (1811 K), J/mol	Method
[1946Smi]	900	...	...	Fe-C phase diagram
[1956Pat]	...	869 ($\pm$175)	15,305 ($\pm$133)	Drop calorimetry
[1959Ole]	...	1150	...	Drop calorimetry
[1960Wal]	911 ($\pm$80)	...	...	Pulse heating
[1962And]	941 ($\pm$80)	1088 ($\pm$210)	...	Drop calorimetry
[1962Fer1]	...	...	**13,807**	Binary phase diagrams
[1962Fer2]	...	1100 ($\pm$293)	13,774 ($\pm$335)	Drop calorimetry
[1963Den]	**900**	**837**	...	Adiabatic calorimetry
[1965Bra]	910 ($\pm$20)	850 ($\pm$30)	14,400 ($\pm$300)	Adiabatic calorimetry
[1966Mor]	...	...	13,799 ($\pm$418)	Drop calorimetry
[1966Vol]	...	...	14,400 ($\pm$200)	Adiabatic calorimetry
[1971Tre]	...	...	13,836 ($\pm$293)	Drop calorimetry
[1972Sal]	923 ($\pm$10)	765 ($\pm$22)	...	Adiabatic calorimetry
[1975Cez]	...	890	...	Pulse heating
[1980Rog]	900 ($\pm$20)	...	...	Adiabatic calorimetry
[1981Sch2]	954	770	14,390	Drop calorimetry
[1982Ben]	820	850	...	Adiabatic calorimetry
[1937Joh]	1339	444	...	Assessment
[1951Dar]	900	690	15,355	Assessment
[1963Kau]	879	937	...	Assessment
[1963Koh]	900	950	...	Assessment
[1967Orr]	900	837	13,807	Assessment
[1973Hul]	900	837	13,807	Assessment
[1979Jon]	1011	825	13,807	Assessment
[1979Sch]	900	820	14,403	Assessment
[1985Gui]	1013	826	13,807	Assessment
[1986Des]	900	850	13,810	Assessment
This work	**900**	**837**	**13,807**	Assessment

entropy difference between the bcc and fcc phases should increase more drastically as temperature is lowed from 1185 to 1000 K (Fig. 10). This can be readily achieved by a steeper decrease of the magnetic entropy in the bcc phase around the Curie temperature 1043 K (Fig. 11). As a matter of fact, a more accurate description of the magnetic heat capacity of bcc iron, such as the one given in the Appendix (Fig. A1 and A2), can meet such a crucial requirement (Fig. 11).

The Gibbs energy and enthalpy differences between bcc and fcc iron over the entire temperature range are shown in Fig. 12. At room temperature, the assessed values on $\Delta H^{bcc/fcc}$ and $\Delta G^{bcc/fcc}$ by [1985Gui] are about 2 and 1 kJ/mol larger than that of the present study, respectively. This is similarly true if the data by [1967Orr] are extrapolated to the lower temperatures. The deviation of [1985Gui] and [1967Orr]'s results from the present work is due to the fact that the heat capacity of the fcc phase cannot be well approximated by a simple linear extrapolation over the low-temperature region (Fig. 5).

Figure 12 also shows the results from [1963Kau], where the lattice stabilities of iron were established with a similar physical background to that used in the present study. In the [1963Kau] assessment, two enthalpy values at 673 and 773 K from [1960Sch] were included in the input data for parameter optimization. As a result, [1963Kau]'s evaluation is very close to the experimental information [1960Sch], which was

obtained by measuring the enthalpy difference in a series Fe-Ni alloys and extrapolating to pure iron. However, [1963Kau] failed to match the data from [1946Smi], which have just been shown in Fig. 8 and 9 to be remarkably consistent with other critical experimental information. Therefore, we conclude that [1960Sch]'s measurements are not in accord with the high-temperature experimental information.

The lattice stabilities of fcc and liquid-amorphous iron is given relative to bcc iron in Fig. 13. The intersection of the lines for the fcc and liquid-amorphous phase is at 1800 K, where fcc iron would melt metastably. This value is in good agreement with the values, 1800 and 1801 K, given by [1967Orr] and [1985Gui], respectively.

The ground-state energy difference between bcc and fcc iron from different work is compared in Table 4. It is clear that the recent *ab initio* values [1999Her, 1997Mor, 1996Cho, 1993Asa, 1991Sin, 1989Bag] are all larger than the data from thermodynamic analysis, but an encouraging trend is also found in that the theoretically predicted values have become smaller and smaller with time. From Table 4, we can also see that the energy-gap (ΔE^{2st}) value obtained for the two magnetic states of fcc iron in this study is in fair agreement with that of [1978Ben] and [1994Ace]. In the assessment of [1963Kau], as we mentioned previously, the low-temperature antiferromagnetic contribution in fcc iron was not considered. Consequently, a smaller value for ΔE^{2st} had to be used in
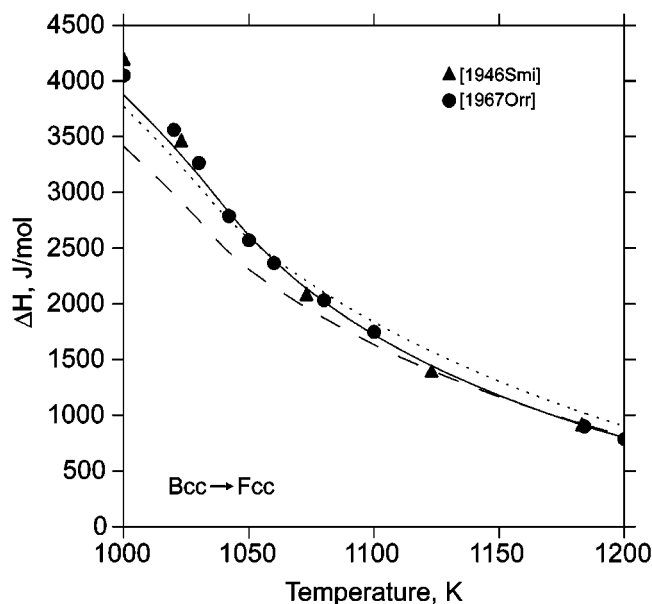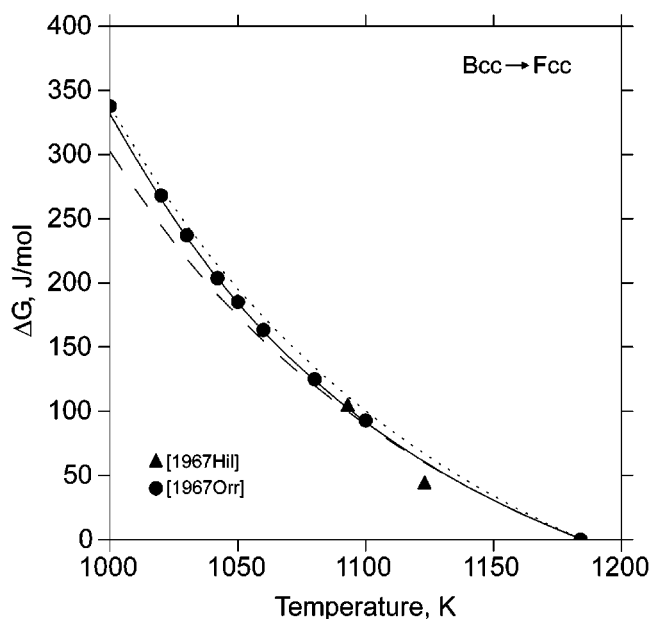
Fig. 8 Comparison between the calculated and experimental data on the enthalpy difference between bcc and fcc iron. The dotted line is from [1985Gui]. The dashed line is from a preliminary assessment where the magnetic contribution was taken the same as in [1985Gui], but the preferred transformation enthalpy value at 1185 K was adopted. The solid line is obtained with the adjusted magnetic model given in the Appendix of this study

order for the extra entropy resulting from the two-state excitation to be large enough to make fcc iron stable at 1185 K.

The treatment of the liquid and amorphous phases as one phase provides a good opportunity to compare the calculated enthalpy of crystallization against the experimental one. From DSC experiments, [2000Sus] estimated that the crystallization enthalpy of pure amorphous iron (at 580 K) is about 15 kJ/mol. Extrapolation from the data on the enthalpy of crystallization of $Fe_{100-y}B_y$ metallic glasses to pure iron suggests a value between 13.8 and 19.21 kJ/mol [1984Ant]. Those values seem to be contrary to the general perception that the enthalpy of crystallization should be smaller than the melting enthalpy, which is 13.807 kJ/mol for iron. However, our calculations also yield a value, 15.93 kJ/mol (at 580 K), in very good agreement with the experimental information. We found that the abnormally large value on the enthalpy of crystallization of amorphous iron is due to the magnetic contribution in amorphous iron.

Conclusions

The thermodynamic properties of pure iron have been constructed from various physical components including lattice, electronic, anharmonic, and magnetic contributions. A relatively more accurate description of the magnetic effect in bcc iron has been suggested, and an accommodation of different experimental measurements on the enthalpy and Gibbs energy differences between bcc and fcc iron has been obtained. The liquid and amorphous phases have been treated as one phase with the generalized two-state model. The calculated crystallization enthalpy of amorphous iron is found to be in good agreement with the experimental data.

(a)
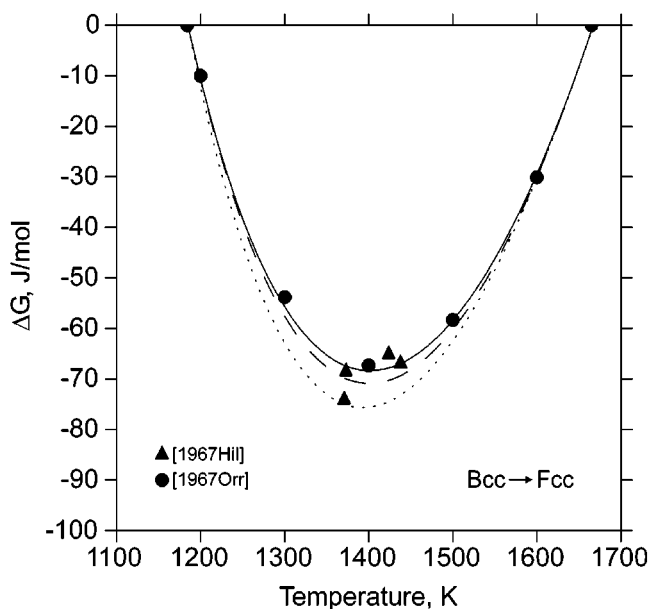
(b)

Fig. 9 Comparison between the calculated and experimental data on the Gibbs energy difference between bcc and fcc iron **(a)** from 1000 to 1185 K and **(b)** from 1185 to 1667 K. The dotted line is from [1985Gui]. The dashed line is from a preliminary assessment where the magnetic contribution was taken the same as in [1985Gui], but the preferred transformation enthalpy value at 1185 K was adopted. The solid line is obtained with the adjusted magnetic model given in the Appendix of this study
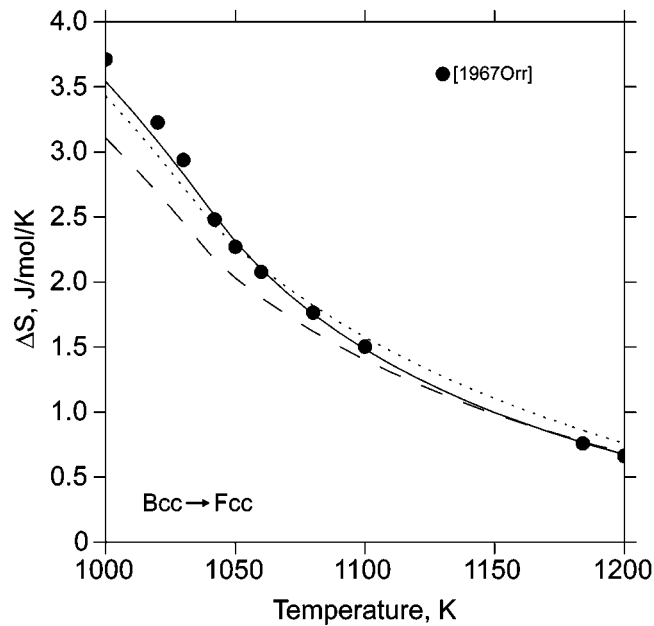
Fig. 10 Comparison between the calculated and experimental data on the entropy difference between bcc and fcc iron 1000 to 1200 K. The dotted line is from [1985Gui]. The dashed line is from a preliminary assessment where the magnetic contribution was taken the same as in [1985Gui], but the preferred transformation enthalpy value at 1185 K was adopted. The solid line is obtained with the adjusted magnetic model given in the Appendix of this study
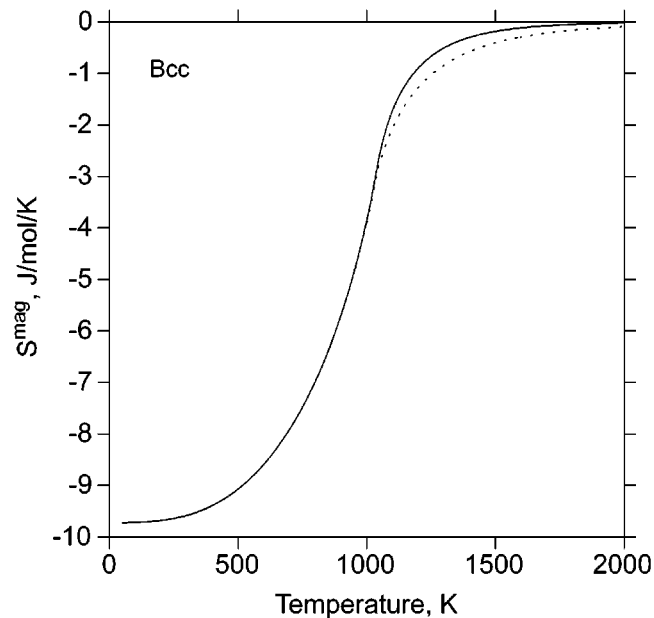

Fig. 11 The magnetic entropy calculated according [1985Gui] (dotted line) and the adjusted model given in the Appendix of this study (solid line)

Appendix

According to [1976Ind], the magnetic heat capacity, C_P^{mag}, can be expressed empirically by
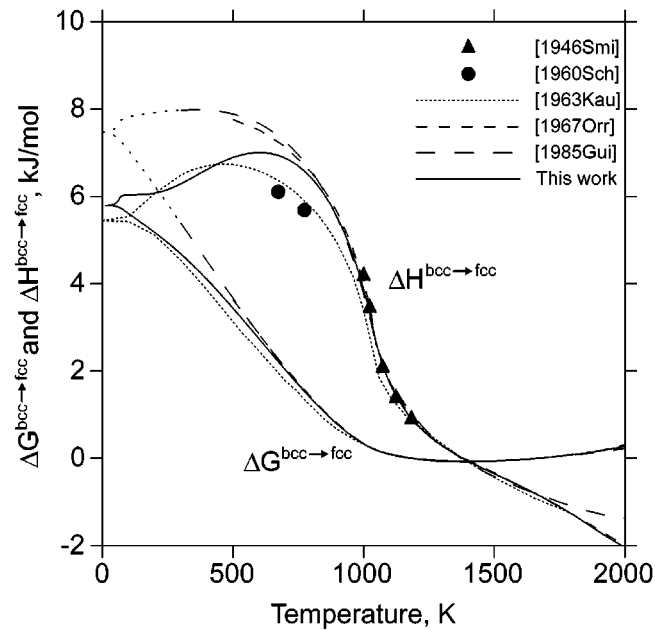

Fig. 12 The enthalpy and Gibbs energy difference between bcc and fcc iron over the entire temperature range
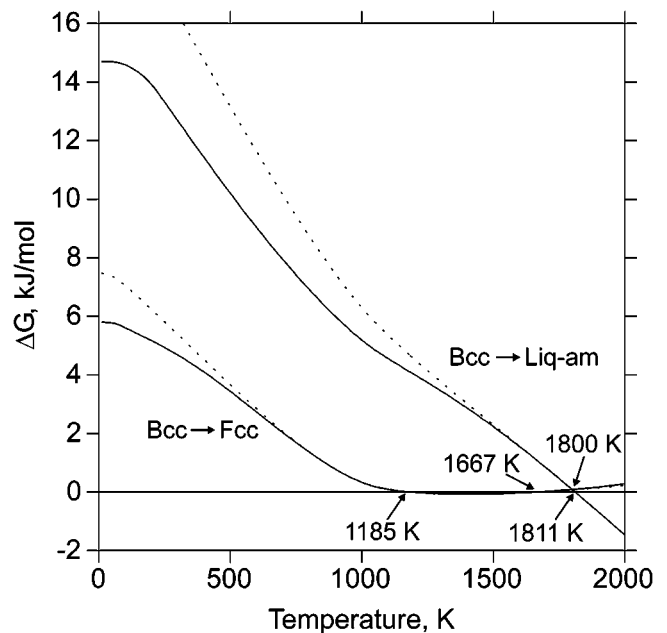

Fig. 13 The calculated lattice stability of iron at 101,325 Pa. The dotted line is from [1985Gui] and the solid line from the present investigation

$$C_P^{\mathrm{mag}} = k^- \, \mathrm{R} \, \ln \frac{1 + \tau^m}{1 - \tau^m} \qquad \tau = \frac{T}{T_C} \leq 1 \qquad \text{(Eq A1)}$$

$$C_P^{\mathrm{mag}} = k^+ \, \mathrm{R} \, \ln \frac{\tau^n + 1}{\tau^n - 1} \qquad \tau = \frac{T}{T_C} > 1 \qquad \text{(Eq A2)}$$

where $m = 3$ and $n = 5$. The quantity, T_C, is the Curie temperature, and the parameters, k^- and k^+, are obtained through the following constraints:

Table 4 The ground state energies for bcc and fcc iron from thermodynamic modeling and calculations

Source	$\Delta E^{\text{bcc}\rightarrow\text{fcc}}(0)$ kJ/mol	ΔE^{2st} kJ/mol	Method
[1999Her]	9.754	5.12	FLAPW
[1999Jam]	…	15	LMTO
[1997Mor]	10.9	…	USPP
[1996Cho]	19.56	…	FLAPW
[1994Ace]	…	11.3	Heat capacity
[1993Asa]	16.02	3.94	LMTO
[1991Sin]	18.25	…	FLAPW
[1989Bag]	14.44	…	LMTO
[1978Ben]	…	10.8	Heat capacity
[1963Kau]	5.44	3.5	Assessment
This work	5.80	9.02	Assessment

$$p = \frac{\int_{T_c}^{\infty} C_P^{\text{mag}}\, dT}{\int_0^{\infty} C_P^{\text{mag}}\, dT} \cong 0.4 \text{ (bcc)}, 0.28 \text{ (fcc)} \qquad \text{(Eq A3)}$$

$$S^{\text{mo}}(\infty) = \int_0^{\infty} \frac{C_P^{\text{mag}}}{T}\, dT = \text{R} \ln(\beta + 1) \qquad \text{(Eq A4)}$$

where p is the fraction of enthalpy for short-range ordering, and it is structure dependent; and β is the average magnetic moment per atom. After Maclaurin expansion of Eq A1 and A2 and retaining the first three terms, [1978Hil] obtained

$$C_P^{\text{mag}} = 2k^- \text{R}\left(\tau^m + \frac{1}{3}\tau^{3m} + \frac{1}{5}\tau^{5m}\right) \qquad \tau = \frac{T}{T_C} \leq 1$$

$$\text{(Eq A5)}$$

$$C_P^{\text{mag}} = 2k^+ \text{R}\left(\tau^{-n} + \frac{1}{3}\tau^{-3n} + \frac{1}{5}\tau^{-5n}\right) \qquad \tau = \frac{T}{T_C} > 1$$

$$\text{(Eq A6)}$$

As explained in the Results and Discussion section, it was found that the preceding descriptions need to be improved for the bcc phase in order to accommodate various experimental information on the enthalpy and Gibbs energy difference between bcc and fcc iron (Fig. 8 to 10).

In order to obtain a possibly better expression, experimental heat capacities of bcc iron were separated into magnetic and paramagnetic parts by using the model outlined in this work. The experimental magnetic heat-capacity data, thus derived, were then used to optimize m, n, k^-, and k^+ in Eq A5 and A6 with the constraint of Eq A4. The obtained m and n are around 3 and 7, respectively, and subsequently, they were fixed to integer values, and the parameters, k^- and k^+, were reoptimized. The obtained optimum values of k^-

and k^+ yielded $p = 0.37$. Finally, one more expansion term was added in Eq A5 and A6 for obtaining an even closer agreement between calculated and experimental $\Delta H^{\text{bcc/fcc}}$ and $\Delta G^{\text{bcc/fcc}}$, as well as the magnetic heat capacities around the Curie temperature.

In conclusion, through a reexamination of the magnetic heat capacity of bcc iron and following the ideas of [1976Ind] and [1978Hil], we obtained

$$C_P^{\text{mag}} = \text{R} \ln(\beta + 1)\left[0.63570895\left(\frac{1}{p} - 1\right)\left(2\tau^3 + \frac{2\tau^9}{3}\right.\right.$$
$$\left.\left. + \frac{2\tau^{15}}{5} + \frac{2\tau^{21}}{7}\right)\right]\bigg/ D \qquad \tau = \frac{T}{T_C} \leq 1 \qquad \text{(Eq A7)}$$

$$C_P^{\text{mag}} = \text{R} \ln(\beta + 1)\left[2\tau^{-7} + \frac{2\tau^{-21}}{3} + \frac{2\tau^{-35}}{5}\right.$$
$$\left. + \frac{2\tau^{-49}}{7}\right]\bigg/ D \qquad \tau = \frac{T}{T_C} > 1 \qquad \text{(Eq A8)}$$

where $D = 0.33471979 + 0.49649686\left(\frac{1}{p} - 1\right)$. Correspondingly, one has

$$G^{\text{mdo}}(\infty) = -\text{R} \ln(\beta + 1)\left[T - 0.38438376\frac{T_C}{pD}\right]$$

$$\text{(Eq A9)}$$

and

$$G^{\text{mo}} = \text{R}\, T \ln(\beta + 1)\, f(\tau) \qquad \text{(Eq A10)}$$

where

$$f(\tau) = 1 - \left[0.38438376\frac{\tau^{-1}}{p} + 0.63570895\left(\frac{1}{p} - 1\right)\right.$$
$$\left.\left(\frac{\tau^3}{6} + \frac{\tau^9}{135} + \frac{\tau^{15}}{600} + \frac{\tau^{21}}{1617}\right)\right]\bigg/ D \qquad \tau \leq 1 \quad \text{(Eq A11)}$$

$$f(\tau) = -\left[\frac{\tau^{-7}}{21} + \frac{\tau^{-21}}{630} + \frac{\tau^{-35}}{2975} + \frac{\tau^{-49}}{8232}\right]\bigg/ D \qquad \tau > 1$$

$$\text{(Eq A12)}$$

For bcc iron, $T_C = 1043$ K, $\beta = 2.22$, and $p = 0.37$. The calculated magnetic heat capacity is compared with that from [1985Gui] and experimental results in Fig. A1 and A2. Apparently, the readjusted form gives closer agreement with the experimental data. The improvement may be marginal, but it is essential in the critical situation of bcc and fcc iron.

Applying Eq A7 through A12 to the fcc structure and keeping the low-temperature C_P^{mag} ($\tau \leq 1$) the same as that of [1978Hil, 1985Gui], $p = 0.25$ can be readily derived. The
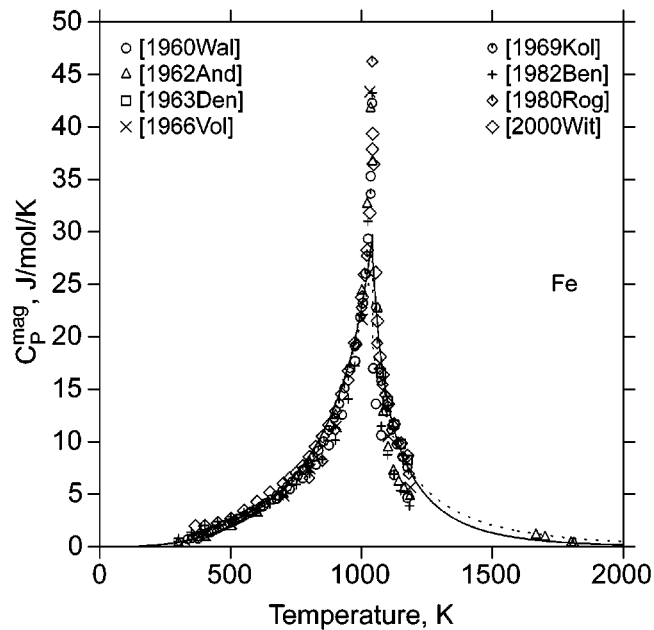
Fig. A1 Comparison between the calculated and experimental magnetic heat capacity of bcc iron. The dashed line is from [1985Gui], and the solid one is obtained using the adjusted model in this study

Fig. A2 A closeup of the comparison between the calculated and experimental magnetic heat capacity of bcc iron. The dashed line is from [1985Gui], and the solid one is obtained using the adjusted model in this study
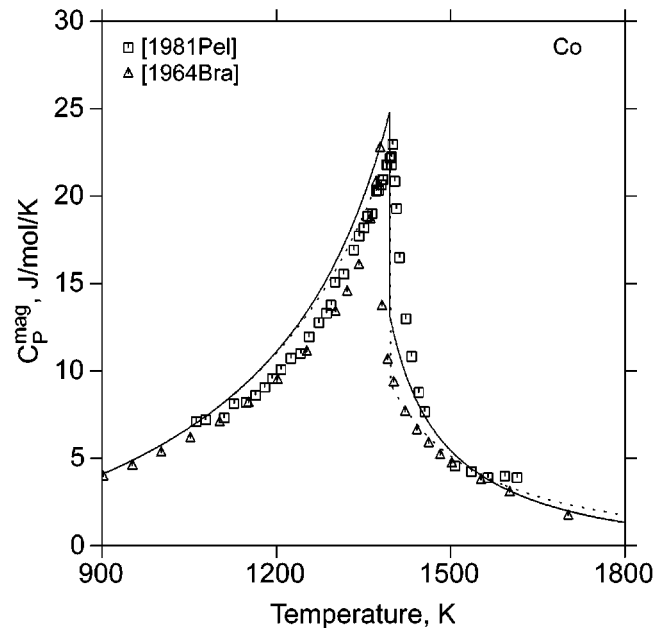
comparisons for Co and Ni are given in Fig. A3 and A4. From these two cases, it is hard to tell whether the original form or the adjusted form is better, although the latter one may give a slight improvement for Co considering the fact that the Curie temperature reported by [1964Bra] is 19 K lower than the accepted value [1987Gui]. Further investigation on other fcc substances or alloys is warranted.

Fig. A3 Comparison between the calculated and experimental magnetic heat capacity of fcc cobalt. The dashed line is from [1987Gui], and the solid one is obtained using the adjusted model in this study
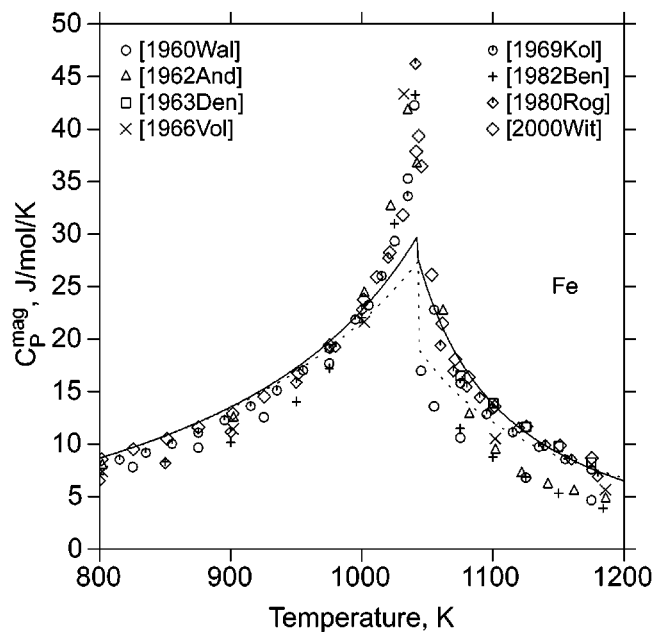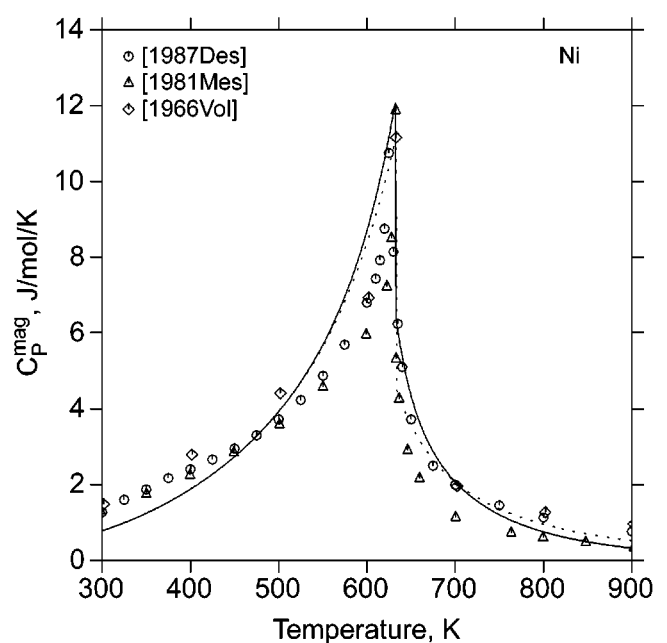

Fig. A4 Comparison between the calculated and experimental magnetic heat capacity of fcc nickel. The dashed line is from [1991Din], and the solid one is obtained using the adjusted model in this study

References

1930Euc: A. Eucken and H. Werth: *Z. Anorg. Allg. Chem.,* 1930, vol. 188, p. 152.
1932Aus: J.B. Austin: *Ind. Eng. Chem.* 1932, vol. 24, p. 1225.
1935Sim: F. Simon and R.C. Swain: *Z. Phys. Chem. Abt. B,* 1935, vol. 28, p. 189.

1937Joh: C.H. Johansson: *Arch. Eisenhuettenwes.,* 1937, vol. 11, p. 241.

1939Kee: W.H. Keesom and B. Kurrelmeyer: *Physica,* 1939, vol. 6, p. 663.

1943Kel: K.K. Kelley: *J. Chem. Phys.,* 1943, vol. 11, p. 16.

1946Smi: R.P. Smith:*J. Am. Chem. Soc.,* 1946, vol. 68, p. 1163.

1946Zen: C. Zener: *Trans. AIME,* 1946, vol. 167, p. 513.

1949Fis: J.C. Fisher: *Trans. AIME,* 1949, vol. 185, p. 688.

1951Dar: L.S. Darken and R.P. Smith: *Ind. Eng. Chem.,* 1951, vol. 43, p. 1815.

1954Bor: M. Born and K. Huang: *Dynamical Theory of Crystal Lattices,* Oxford University Press, Oxford, United Kingdom, 1954.

1955Zen: C. Zener: *Trans. AIME,* 1955, vol. 203, p. 619.

1956Hof: J.A. Hofmann, A. Paskin, K.J. Tauer, and R.J. Weiss: *J. Phys. Chem. Solids,* 1956, vol. 1, p. 45.

1956Pat: J.R. Pattison and P.W. Willows: *J. Iron Steel Inst.,* 1956, vol. 183, p. 390.

1956Wei: R.J. Weiss and K.J. Tauer: *Phys. Rev.,* 1956, vol. 102, p. 1490.

1959Arp: V. Arp, D. Edmonds, and R. Petersen: *Phys. Rev. Lett.,* 1959, vol. 3, p. 212.

1959Ole: M. Olette and A. Ferrier: *The Physical Chemistry of Metallic Solutions and Intermetallic Compounds,* Symposium No. 9, Paper 4H, National Physical Laboratory, Teddington, England, 1959, pp. 100-09.

1960Che: C.H. Cheng, C.T. Wei, and P.A. Beck: *Phys. Rev.,* 1960, vol. 120, p. 426.

1960Sch: E. Scheil and E. Saftig: *Arch. Eisenhuettenwes.,* 1960, vol. 31, p. 623.

1960Wal: D.C. Wallace, P.H. Sidles, and G.C. Danielson: *J. Appl. Phys.,* 1960, vol. 31, p. 168.

1962And: P.D. Anderson and R. Hultgren: *Trans. AIME,* 1962, vol. 224, p. 842.

1962Fer1: A. Ferrier: *C. R. Acad. Sci.,* 1962, vol. 254, p. 104.

1962Fer2: A. Ferrier and M. Olette: *C. R. Acad. Sci.,* 1962, vol. 254, p. 2322.

1963Den: W.A. Dench and O. Kubaschewski: *J. Iron Steel Inst.,* 1963, vol. 201, p. 140.

1963Hul: R. Hultgren, R.L. Orr, P.D. Anderson, and K.K. Kelley: *Selected Values of Thermodynamic Properties of Metals and Alloys,* John Wiley, New York, NY, 1963.

1963Kau: L. Kaufman, E.V. Clougherty, and R.J. Weiss: *Acta Metall.,* 1963, vol. 11, p. 323.

1963Koh: R. Kohlhaas and M. Braun: *Arch. Eisenhuettenwes.,* 1963, vol. 34, p. 391.

1963Wei: R.J. Weiss: *Proc. Phys. Soc.,* 1963, vol. 82, p. 281.

1964Bra: M. Braun and R. Kohlhaas: *Z. Naturforschg.,* 1964, vol. 19a, p. 663.

1964Gup: K.P. Gupta, C.H. Cheng, and P. Beck: *J. Phys. Chem. Solids,* 1964, vol. 25, p. 73.

1965Bra: M. Braun and R. Kohlhaas: *Phys. Status Solidi,* 1965, vol. 12, p. 429.

1966Mor: J.P. Morris, E.F. Foerster, C.W. Schultz, and G.R. Zellars: U.S. Bureau of Mines Report Investigation No. 6723, U.S. Government Printing Office, Washington, DC, 1966.

1966Shi: S.S. Shinozaki and A. Arrott: *Phys. Rev.,* 1966, vol. 152, p. 611.

1966Vol: O. Vollmer, R. Kohlhaas, and M. Braun: *Z. Naturforschg.,* 1966, vol. 21A, p. 181.

1967Che: H.S. Chen and D. Turnbull: *J. Appl. Phys.* 1967, vol. 38, p. 3646.

1967Hil: M. Hillert, T. Wada, and H. Wada: *J. Iron Steel Inst.,* 1967, vol. 205, p. 539.

1967Orr: R.L. Orr and J. Chipman: *Trans. AIME,* 1967, vol. 239, p. 630.

1968Ste: G.L. Stepakoff and L. Kaufman: *Acta Metall.,* 1968, vol. 16, p. 13.

1969Kol: T.G. Kollie, M. Barisoni, D.L. McElroy, and C.R. Brooks: *High Temp.-High Pressures,* 1969, vol. 1, p. 167.

1970Kau: L. Kaufman and H. Bernstein: *Computer Calculation of Phase Diagrams,* Academic Press, New York, NY, 1970.

1970Mio: A.P. Miodownik: *Acta Metall.,* 1970, vol. 18, p. 541.

1971Mar: K. Marklund, L. Hoel, K. Spahr, and T. Lindqvist: *J. Low Temp. Phys.,* 1971, vol. 5, p. 227.

1971Tan: Y. Tanji: *J. Phys. Soc. Jpn.,* 1971, vol. 30, p. 133.

1971Tre: J.A. Treverton and J.L. Margrave: *J. Chem. Thermodyn.,* 1971, vol. 3, p. 473.

1972Chi: J. Chipmanl: *Metall. Trans.,* 1972, vol. 3, p. 55.

1972Sal: F.R. Sale and A.S. Normanton: in *Metallurgical Chemistry Symposium 1971,* National Physical Laboratory, Teddington, England, 1972, pp. 19-28.

1973Hul: R. Hultgren, P.D. Desai, D.T. Hawkins, M. Gleiser, K.K. Kelley, and D.D. Wagman: *Selected Values of Thermodynamic Properties of Metals and Alloys,* American Society of Metals, Metals Park, OH, 1973.

1974Cez: A. Cezairliyan and J.L. McClure: *J. Res. Nat. Bur. Stand. Sect. A,* 1974, vol. 78, p. 1.

1974Gri: G. Grimvall: *Solid State Commun.,* 1974, vol. 14, p. 551.

1974Red: B.P.N. Reddy and P.J. Reddy: *Phys. Status Solidi A,* 1974, vol. 22, p. 219.

1975Cez: A. Cezairliyan and J.L. McClure: *High Temp. Sci.,* 1975, vol. 7, p. 189.

1975Hau: G. Hausch: *Phys. Stat. Sol. A,* 1975, vol. 30, p. K57.

1976Hei: N. Heiman, K. Lee, R.I. Potter, and S. Kirkpatrick: *J. Appl. Phys.,* 1976, vol. 47, p. 2634.

1976Ind: G. Inden: *Proc. Project Meeting CALPHAD V,* Duesseldorf, Germany, 1976, p. III.4-1.

1977Fuk: K. Fukamichi, M. Kikuchi, S. Arakawa, and T. Masumoto: *Solid State Commun.,* 1977, vol. 23, p. 955.

1977Mio: A.P. Miodownik: *CALPHAD,* 1977, vol. 1, p. 133.

1978Ben: W. Bendick, H.H. Ettwig, and W. Pepperhoff: *J. Phys. F,* 1978, vol. 8, p. 2525.

1978Has: R. Hasegawa and R. Ray: *J. Appl. Phy.,* 1978, vol. 49, p. 4174.

1978Hil: M. Hillert and M. Jarl: *CALPHAD,* 1978, vol. 2, p. 227.

1978Hir: H. Hiroyoshi, K. Fukamichi, M. Kikuchi, A. Hoshi, and T. Masumoto: *Phys. Lett.,* 1978, vol. 65A, p. 163.

1978Kaz: N.S. Kazama, N. Heiman, and H. Watanabe: *Suppl. Sci. Rep. RITU A,* 1980, p. 131.

1978Lub: F.E. Luborski, H.H. Liebermann, J.J. Becker, and J. Walter: *Proc. 3rd Int. Conf. on Rapidly Quenched Metals,* The Metals Society, London, 1978, vol. 2, p. 188.

1979Ågr: J. Ågren: *Metall. Trans. A,* 1979, vol. 10A, p. 1847.

1979Sch: E. Schurmann and V. Neubert: *Arch. Eisenhuettenwes.,* 1979, vol. 50, p. 415.

1980Mas: T. Masumoto, S. Ohnuma, K. Shirakawa, M. Nose, and K. Kobayashi: *J. Phys.,* 1980, vol. 41, p. C8-686.

1980Rog: J. Rogez and J. Le Coze: *Rev. Phys. Appl.,* 1980, vol. 15, p. 341.

1981Bus: K.H.J. Buschow and P.G. van Engen: *J. Appl. Phys.,* 1981, vol. 52, p. 3557.

1981Chi: C.L. Chien and K.M. Unruh: *Phys. Rev.* 1981, vol. B24, p. 1556.

1981Fuk: K. Fukamichi and R.J. Gambino: *IEEE Trans. Magn.,* 1981, vol. 17, p. 3059

1981Mes: P.J. Meschter, J.W. Wright, and C.R. Brook: *J. Phys. Chem. Solids,* 1981, vol. 42, p. 861.

1981Pel: V.E. Peletskii and E.B. Zaretskii: *High Temp.-High Pressure,* 1981, vol. 13, p. 661.

1981Sch1: H.R. Schober and P. H. Dederichs: in *Landolt-Börnstein Numerical Data and Functional Relationships in Science and*

Technology New Series, III/13a, K.H. Hellwege and J.L. Olsen, eds., Springer, Berlin, 1981, p. 55.

1981Sch2: E. Schurmann and H.P. Kaiser: *Arch. Eisenhuettenwes.,* 1981, vol. 52, p. 99.

1982Ben: W. Bendick and W. Pepperhoff: *Acta Metall.,* 1982, vol. 30, p. 679.

1982Fuk: K. Fukamichi, H. Hiroyoshi, T. Kaneko, T. Masumoto, and K. Shirakawa: *J. Appl. Phys.,* 1982, vol. 53, p. 8107.

1983Bay: G. Bayreuther, G. Enders, H. Hoffmann, U. Korndörfer, W. Oestreicher, K. Röll, and M. Takahashi: *J. Magn. Magn. Mater.,* 1983, vol. 31-34, p. 1535.

1983Shi: K. Shirakawa, K. Fukamichi, T. Kaneko, and T. Masumoto: *Sci. Rep. RITU A,* 1983, vol. A31, p. 54.

1984Ant: C. Antonione, L. Battezzati, G. Cocco, and F. Marino: *Z. Metallkd.,* 1984, vol. 75, p. 714.

1984Ega: T. Egami: *Rep. Prog. Phys.*, 1984, vol. 47, p. 1601.

1984Jan: B. Jansson: Ph.D. Thesis, Royal Institute of Technology, Stockholm, 1984.

1984Per: J.H. Perepezko and J.S. Paik: *J. Non-Cryst. Solids,* 1984, vol. 61-62, p. 113.

1985Chi: C.L. Chien, S.H. Liou, B.K. Ha, and K.M. Unruh: *J. Appl. Phys.,* 1985, vol. 57, p. 3539.

1985Cow: N. Cowlam and G. E. Carr: *J. Phys. F,* 1985, vol. 15, p. 1109.

1985Gui: A.F. Guillermet and P. Gustafson: *High Temp.-High Pressure,* 1985, vol. 16, p. 591.

1985Lio: S.H. Liou, G. Xiao, J.N. Taylor, and C.L. Chien: *J. Appl. Phys.,* 1985, vol. 57, p. 3536.

1985Sun: B. Sundman, B. Jansson, and J.-O. Andersson: *CALPHAD,* 1985, vol. 9, p. 153.

1986Des: P.D. Desai: *J. Phys. Chem. Ref. Data,* 1986, vol. 15, p. 967.

1986Gri: G. Grimvall: *Thermophysical Properties of Materials,* Elsevier Science, North-Holland, Amsterdam, 1986.

1987And: J.-O. Andersson, A.F. Guillermet, P. Gustafson, M. Hillert, B. Jansson, B. Jonsson, B. Sundman, and J. Ågren: *CALPHAD,* 1987, vol. 11, p. 93.

1987Des: P.D. Desai: *Int. J. Thermophys.,* 1987, vol. 8, p. 763.

1987Gui: A.F. Guillermet: *Int. J. Thermophys.,* 1987, vol. 8, p. 481.

1987Her: U. Herr, J. Jing, R. Birringer, U. Gonser, and H. Gleiter: *Appl. Phys. Lett.,* 1987, vol. 50, p. 472.

1988Car: C. Carbone, G.S. Sohal, E. Kisker, and E.F. Wassermann: *J. Appl. Phys.,* 1988, vol. 63, p. 3499.

1988Ågr: J. Ågren: *Phys. Chem. Liq.,* 1988, vol. 18, p. 123.

1989Bag: P. Bagno, O. Jepsen, and O. Gunnarsson: *Phys. Rev. B,* 1989, vol. 40, p. 1997.

1989Ken: W. Keune, T. Ezawa, W.A.A. Macedo, U. Glos, K.P. Schletz, and U. Kirschbaum: *Physica B,* 1989, vol. 161, p. 269.

1991Din: A.T. Dinsdale: *CALPHAD,* 1991, vol. 15, p. 317.

1991Ind: G. Inden: *Scand. J. Metall.,* 1991, vol. 20, p. 112.

1991Kau: L. Kaufman: *Scand. J. Metall.,* 1991, vol. 20, p. 32.

1991Sin: D.J. Singh, W.E. Pickett, and H. Krakauer: *Phys. Rev. B,* 1991, vol. 43, p. 11628.

1991Sus: K.S. Suslick, S.-B. Choe, A.A. Cichowlas, and M.W. Grinstaff: *Nature,* 1991, vol. 353, p. 414.

1992Gup: N. Gupta, K.C. Jain, A. Pratap, and N.S. Saxena: *Can. J. Phys.,* 1992, vol. 70, p. 627.

1992Yan: K. Yano, E. Kita, K. Tokumitsu, H. Ino, and A. Tasaki: *J. Magn. Mag. Mater.,* 1992, vol. 104-107, p. 131.

1993Asa: T. Asada and K. Terakura: in *Computer Aided Innovation of New Materials,* M. Doyama, J. Kihara, M. Tanaka, and R. Yamamoto, eds., Elsevier Publ., North-Holland, Amsterdam, 1993, pp. 169-72.

1993Bar: M. Barth, F. Joo, B. Wei, and D.M. Herlach: *J. Non-Cryst. Solids,* 1993, vol. 156-158, p. 398.

1993Bel: R. Bellissent, G. Galli, M.W. Ginstaff, P. Migliardo, and K.S. Suslick: *Phys. Rev. B,* 1993, vol. 48, p. 15797.

1993Gri: M.W. Grinstaff, M.B. Salamon, K.S. Suslick: *Phys. Rev. B,* 1993, vol. 48, p. 269.

1994Ace: M. Acet, H. Zähres, E.F. Wassermann, and W. Pepperhoff: *Phys. Rev. B,* 1994, vol. 49, p. 6012.

1994Gho: G. Ghosh and G.R. Olson: *Acta Metall. Mater.,* 1994, vol. 42, p. 3371.

1994Wei: B. Wei, B. Wang, M. Barth, D.M. Herlach: *Acta Metall. Sinica,* 1994, vol. 30, p. B289.

1995Ågr: J. Ågren, B. Cheynet, M.T. Clavaguera-Mora, K. Hack, J. Hertz, F. Sommer, and U. Kattner: *CALPHAD,* 1995, vol. 19, p. 449.

1995Bel: R. Bellissent, G. Galli, T. Hyeon, S. Magazu, D. Majolino, P. Migliardo, and K.S. Suslick: *Phys. Scripta,* 1995, vol. 57, p. 79.

1995Cha: M.W. Chase, I. Ansara, A. Dinsdale, G. Eriksson, G. Grimvall, L. Höglund, and H. Yokokawa: *CALPHAD,* 1995, vol. 19, p. 437.

1995Fon: D. de Fontaine, S.G. Fries, G. Inden, P. Miodownik, R. Schmid-Fetzer, and S.-L. Chen: *CALPHAD,* 1995, vol. 19, p. 499.

1995Sch: K. Schaefers, M. Rösner-Kuhn, and M.G. Frohberg: *Mater. Sci. Eng. A,* 1995, vol. 197, p. 83.

1995Sun: B. Sundman and F. Aldinger: *CALPHAD,* 1995, vol. 19, p. 433.

1996Cho: J.-H. Cho and M. Scheffler: *Phys. Rev. B,* 1996, vol. 53, p. 10685.

1996Kit: C. Kittel: *Introduction to Solid State Physics,* John Wiley & Sons, New York, NY, 1996.

1996Lie: M. Liebs and M. Fähnle: *Phys. Rev. B,* 1996, vol. 53, p. 14012.

1997Cac: G. Cacciamani, Y.A. Chang, G. Grimvall, P. Franke, L. Kaufman, P. Miodownik, J.M. Sanchez, M. Schalin, and C. Sigli: *CALPHAD,* 1987, vol. 21, p. 219.

1997Mor: E.G. Moroni, G. Kresse, J. Hafner, and J. Furthmuller: *Phys. Rev. B,* 1997, vol. 56, p. 15629.

1998Hil: M. Hillert: *Phase Equilibrium, Phase Diagrams and Phase Transformations,* Cambridge University Press, New York, NY, 1998.

1998Lon: G.J. Long, D. Hautot, Q.A. Pankhurst, D. Vandormael, F. Grandjean, J.P. Gaspard, V. Briois, T. Hyeon, and K.S. Suslick: *Phys. Rev. B,* 1998, vol. 57, p. 10716.

1998Sau: N. Saunders and A.P. Miodownik: *CALPHAD Calculation of Phase Diagrams: A Comprehensive Guide,* Pergamon, New York, NY, 1998.

1999Her: H.C. Herper, E. Hoffmann, and P. Entel: *Phys. Rev. B,* 1999, vol. 60, p. 3839.

1999Jam: P. James, O. Eriksson, B. Johansson and I.A. Abrikosov: *Phys. Rev. B,* 1999, vol. 59, p. 419.

2000Che: Q. Chen and B. Sundman: Royal Institute of Technology, Stockholm, unpublished work, 2000.

2000Sus: K.S. Suslick: University of Illinois at Urbana-Champaign, Urbana, IL, private communication, 2000.

2000Wit: V.T. Witusiewicz, F. Sommer, and E. Mittemeijer: private communication, 2000.

2001Che: Q. Chen and B. Sundman: *Acta Mater.,* 2001, vol. 49, p. 947.